京都大学防災研究所年報 第46号 B 平成15年
Annuals of Disas. Prev. Res. Inst., Kyoto Univ., No. 46 B, 2003

Parallel Computation of Coupled Atmosphere and Ocean Model -The Case Study of Typhoon 9918 in the Yatsushiro Sea

Kyeongok KIM* and Takao YAMASHITA

* Graduate School of Engineering, Kyoto University

Synopsis

The coupled parallel atmosphere and ocean model was developed and verified in Linux Beowulf system. The hindcast of storm surge caused by Typhoon Bart (T9918) was tested in this system. Computed sea surface changes successfully simulated the observed ones at Yatsushiro Harbour. However, the model underestimated in maximum water elevation at Matsuai (at the northern end of the Yatsushiro Sea). We hope a more comprehensive coupled model considering air-sea-wave interaction may fill this gap.

Keywords: Storm surge, parallel computation, coupled atmosphere and ocean model, Typhoon Bart (T9918)

1. Introduction

Ocean-atmospheric interactions are very important in the formation and development of tropical storms. These interactions are dominant in exchanging heat, momentum, and moisture fluxes. Heat flux is usually computed using a bulk equation. In this equation air-sea interface supplies heat energy to the atmosphere and to the storm. Dynamical interaction is most often one way in that it is the atmosphere that drives the ocean. The winds transfer momentum to both ocean surface waves and ocean current. The wind wave makes an important role in the exchange of the quantities of motion, heat and a substance between the atmosphere and the ocean.

Storm surges can be considered as the phenomena of mean sea-level changes, which are the result of the frictional stresses of strong winds blowing toward the land and causing the set level "set up", as much as several meters under the meteorological disturbances such as typhoon, hurricane, cyclone and gale. The low atmospheric pressure at the center of the cyclone can additionally raise the sea level (the "inverted barometer effect"). In addition to the rise in water level itself, another factor must be considered. A rise of mean sea level due to wave set up should be considered. A 2-3 meters wave set up due to large surface gravity waves associated with the storm may result in disastrous beach erosion of low coast. In bounded bodies of water, such as small seas, wind-

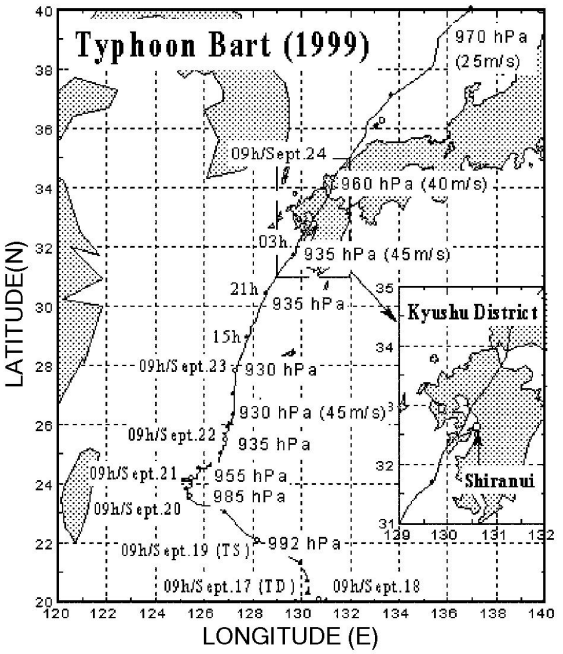

Figure 1. The track of Typhoon Bart (T9918). A broken line indicates a stage of a tropical depression. Date and time are represented by JST. Values on the right-hand side of the track are the central atmospheric pressure and the maximum wind speed.

driven sea level set up is much serious than inverted barometer effects, in which the effects of wind waves on wind-driven current play an important role. It is necessary to develop the coupled system of the full spectral third-generation wind-wave model (WAVEWATCH III), the meso-scale atmosphere model (MM5) and the coastal ocean model (POM) for simulating these physical interactions. As the components of coupled system is so heavy for personal usage, the parallel computing system have to be developed.

In this research, first of all, we developed the coupling system of the atmosphere model and the coastal ocean model, excluding the wind-wave model, in the Beowulf System, for the simulation of the storm surge caused by Typhoon Bart (T9918) in the Yatsushiro Sea. The fundamental perform examination about the applicability of parallel computing efficiency was also carried out.

Typhoon Bart (T9918) was in the Okinawa district moving north slowly, from September 19th to 23rd, and moved in the East China Sea to the northeast, then passed along the Sea of Japan. After landing on northern Kyushu in the morning of the 24th, and moved to Hokkaido on 25th.

Since the typhoon landed at Kyushu with maintaining strong influence a storm and heavy rain attached various places, and the serious high tide calamity caused it in the Shiranui village of Matsuai (Fig. 4). The strong wind blew in the wide area with approach and passage of a typhoon, especially, south wind blew strongly and there were places where observed the storm of 30 or more m/s. Those are southwest islands, or the Kyushu district and the Chugoku district. Maximum instantaneous wind speed 66.2 m/s was observed at the Ushibuka meteorological station of Kumamoto Prefecture. It was a record of the fastest wind since a statistics start of this meteorological station, 1969.

Storm surge occurred in the Yatsushiro Sea and the Ariake Sea on the early morning of the 24th when the typhoon went the Amakusa Area. In Matsuai, storm surge and the high wave flowed into colonies, and took its toll of 12-death. According to the field survey performed later, in the Yatsushiro Sea, the maximum of tide anormaly was presumed to exceed about 3.5m.

Many researches have been dove about Typhoon Bart and its storm surge event. It is studied an analysis of atmospheric pressure pattern in Typhoon Bart by an objective method and compared the gradient wind with the observed surface wind (Fujii et al., 2002). The storm surge induced by Typhoon 9918 in the Yatsushiro Sea is studied and compared with Typhoon 9119 (Manda and Yanagi, 2001). We have calculated the numerical hindcast of storm surge caused by the Typhoon Bart in the Yatsushiro Sea in the previous research (Yamashita and Nakagawa, 2001). That is conducted by storm surge simulation system which consists of a quasi-three-dimensional hydrodynamic model (POM), together with the third-generation ocean wave prediction model (WAM) and Mitsuta's typhoon model.

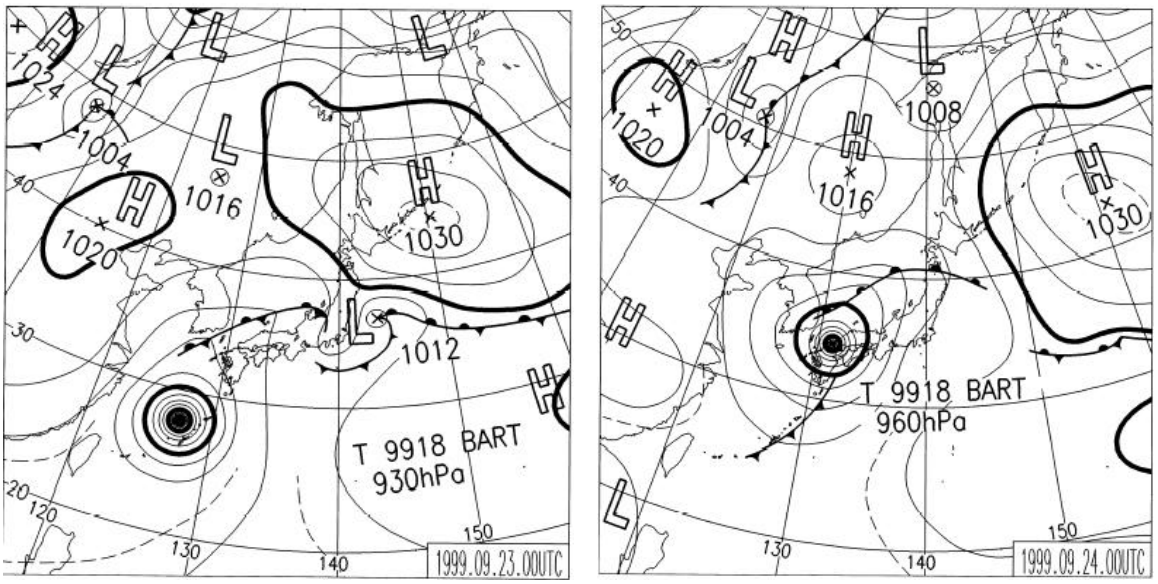

Figure 2. The atmospheric pressure distribution chart of JMA during Typhoon Bart event at (a) 00 UTC 23 (09 JST 23, left) and (b) 00 UTC 24 September (09 JST 24, right).

2. Model Description

The model, modified to execute for coupled parallel run, composed by an atmosphere model, a ocean model and a coupler which transport and interpolate data. The atmosphere and ocean models used are MM5 and POM of MPI version. We developed the coupler and coupling subroutines to archive the parallel system in which each model is executed at same time and these calculate own jobs and pass data with organic system.

2.1 *Mesoscale atmosphere model*

The Pennsylvania State University and National Center for Atmospheric Research have developed the Mesosclae Model (MM5) which is a nonhydrostatic, primitive equation model with a terrain-following coordinate (Grell et al, 1994). In the present study, two nested computational domains are employed. The first and the second domain have grid increments of 9 at 31:30°N, 130°E, covered West Japan and South km and 3km, respectively. The first domain, centered Korea (Figure 3). The two-way nested second domain covers Ariake and Yatsushiro area, and exchange computed value with coupler. Calculations for each domain are performed for mesh sizes of 91×91 points, and time steps of 20 and 6.67 seconds, respectively. 23 vertical full-sigma levels are used from surface pressure level to 100 hPa in all domains. The initial and lateral boundary conditions for the first domain are imposed by the datasets of Japan Meteorological Agency's Regional 20×20 km resolution analyses (JMA-RANAL), which include a typhoon bogussing. These datasets are also used as the initial and boundary conditions of the operational regional spectral model (JMA-RSM) over East Asia. The sea surface temperature field is provided by the weekly 1.0×1.0 degree resolution optimum interpolation SST analysis (Reynolds and Smith 1994), and is held constant throughout the whole periods in all simulations. Model is initialized at 09 JST 22 September, 1999 by JMA-RANAL, and the analysis nudging is used in all experiments, these data verified in the simulation about Typhoon Bart of Yoshino et al. (2002).

The explicit moisture scheme used Reisner groupel shceme that based on mixed-phase shceme but adding gaupel and ice number concentration prediction equations. The mixed-phase microphysics scheme of Reisner et al. (1998) for resolvable scale motions, in which five prognostic equations were used for water vapor, cloud water, rainwater, cloud ice and snow. The high-resolution Blackadar planetary boundary layer (PBL) scheme was used to calculate the vertical fluxes of sensible heat, moisture and momentum.

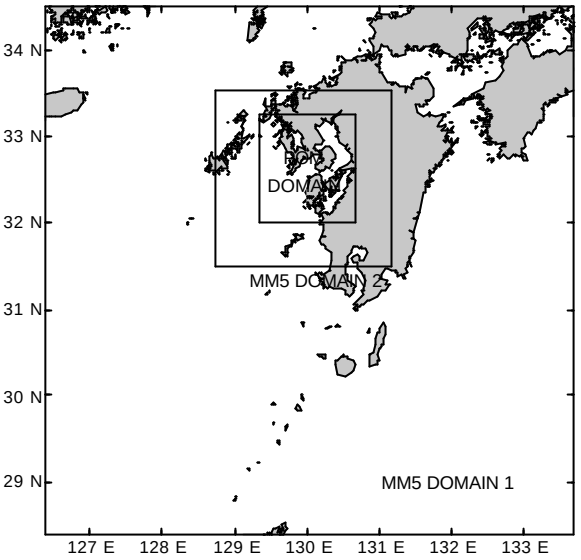

Figure 3. Map of the West Japan area and the first domain used in the atmosphere model. The large square indicates the second domain of the atmosphere model nested in the first domain and the small square is the Ariake and Yatsushiro Seas domain used in ocean model.

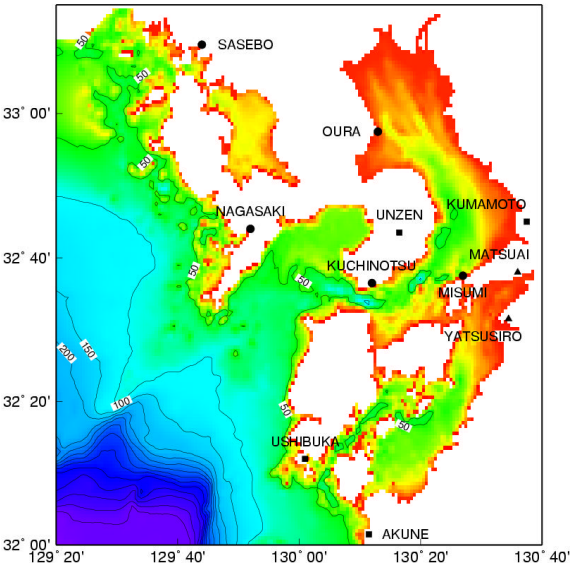

Figure 4. Finite-difference grid for the ocean model (POM) of the West Kyushu, with locations of 5 tide gauges indicated with circles (Sasebo, Nagasaki, Kuchinotsu, Misumi and Oura), 2 damaged districts from the storm surge by Typhoon Bart with triangles (Yatsusiro and Matsuai) and 4 meteorological observation stations with squares (Akune, Kamamoto, Unzen and Ushibuka).

2.2 *Three-dimensional primitive equation ocean model*

The basic equations consisting of the continuity, momentum, hydrostatic, temperature, salinity and density equations of the three-dimensional primitive s-coordinate model are given by

$$u_x + v_y + w_z = 0 \tag{1}$$

$$u_t + uu_x + vu_y + wu_z - fv = -r_0^{-1} p_x + (K_M u_z)_z + F^u \tag{2}$$

$$v_t + uv_x + vv_y + wv_z + fu = -r_0^{-1} p_y + (K_M v_z)_z + F^v \tag{3}$$

$$r g = -p_z \tag{4}$$

$$q_t + uq_x + vq_y + wq_z = (K_H q_z) + F^q \tag{5}$$

$$r = r(q) \tag{6}$$

where (u, v, w) are the velocity components in the (x, y, z) directions, respectively, p the pressure, q the temperature or the salinity, r in situ density, r_0 (=const.) the reference density, f the Coriolis parameter, g the acceleration due to gravity, K_M the vertical eddy viscosity, K_H the vertical eddy diffusivity, $F^{(u,v)}$ the horizontal eddy friction terms, and F^q the horizontal eddy diffusion terms. The K_M and K_H are determined by Mellor and Yamada's level 2.5 turbulence closure model (Mellor and Yamada, 1982). The horizontal friction and diffusion terms are given by Smagorinsky nonlinear viscosity. The model first transforms (1)-(6) into the sigma coordinate system defined by $s = (z-h)/(H-h)$, where h and H are the surface elevation and the water depth, respectively. The resulting equations are splite into the external (vertically averaged) and the internal (three-dimensional) modes toe solve by the mode splitting method (originally developed by Simons; 1980). The Asselin filter is used at every time step to prevent a zigzag solution in time associated with the leapfrog scheme.

The problem is closed by relating bottom stress, t_b, to the depth mean current, U, using a quadratic law

$$t_b = r C_z U|U| \tag{7}$$

where C_z is a coefficient of bottom friction and will increase in value when wave effects are present. This value can be obtained by the following expression (Mellor, 1998),

$$C_z = MAX\left[\frac{k^2}{\ln\left(\left(1+s_{kb-1}\right)H/z_0\right)^2}, 0.0025\right] \tag{8}$$

where $k = 0.4$ is the von Karman constant and H is representative wave height, s_{kb-1} the height of the first grid point near the bottom, z_0 is the roughness parameter. Relating the wind stress, t_s, to the mean surface (10 meter) wind velocity, W, a quadratic low is also used, as,

$$t_s = r_a C_D W|W| \tag{9}$$

where r_a is the density of air and C_D a drag coefficient. The relationship between C_D and W suggested by Smith and Banke (1975)

$$C_D \times 10^3 = 0.63 + 0.066 \times W \tag{10}$$

The model computed by the horizontal grid size of 30 arc-second (about 900 meters) and the time step in internal mode of 10 seconds. The water depth data was interpolated from 500 meter bathymetric database of JODC. The tidal elevation in open boundary was interpolated by the observed data at tide gauges stations closed in the boundary (Sasebo and Akune) and modified to improve the reappearance of tide in the Ariake Sea for eight constituents (M_2, S_2, K_1, O_1, K_2, N_2, P_1, and Q_1). (Kim and Yamashita, 2002)

2.3 *Parallelization of coupled atmosphere and ocean model using SPMD / MPMD*

The Fifth-Generation NCAR / Penn State Mesoscale Model (MM5) and Princeton Ocean Model (POM) have been already made on the parallel codes by the Single Program Multiple Data (SPMD) methods. SPMD means the parallel method that same program runs on each processor.

Each parallel model was tested in the Linux Beowulf system constituted in the Research Center for Disaster Environment, DPRI, Kyoto University, (Pentium4-1.9G 4 nodes, Pentium4-2G 16 nodes and 1 fileserver; totally 21 nodes) and these models have an effect on speedup of 2.7 (POM) and 4.45 (MM5) on 8 processors (Table 1). Figure 5 shows the speedup rate versus the number of CPU. For getting the best performance for computation, we distributed CPU to MM5 with 16 nodes, POM with 4 nodes and the coupler with 1 node.

Table 1. Computation time (wall clock) of models and speedup rate.

# CPU	POM comp. Time (Hr)	MM5 comp. time (Hr)	POM Speedup	MM5 Speedup
1	10.8	39.6	1.00	1.00
2	8.3	22.9	1.30	1.73
4	5.7	14.1	1.89	2.80
8	4.0	8.9	2.70	4.45
16	2.7	6.4	4.00	6.19

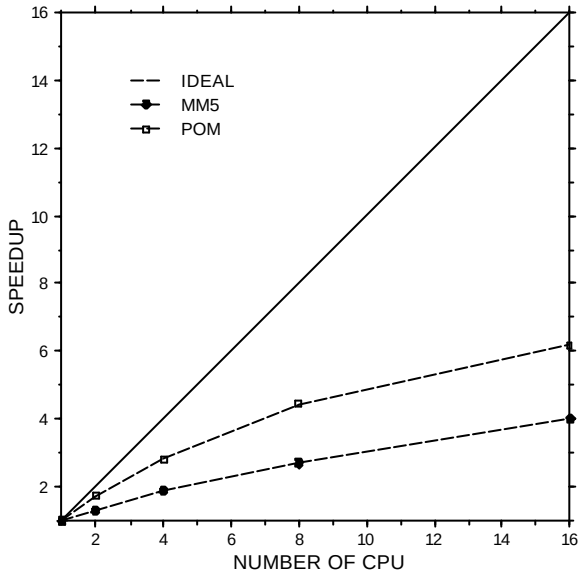

Figure 5. The speedup rates versus the number of CPU with parallel models.

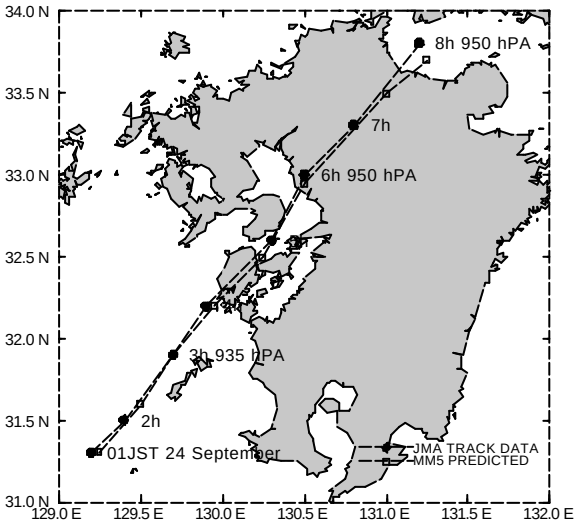

Figure 6. The track of Typhoon Bart between 01 JST 24 September and 08 JST 24 September in Kyushu area. The solid line indicates observed typhoon track and center by JMA and the dotted line the computed typhoon track and center by MM5.

The essential function of the coupler is to repeatedly transfer data, such as atmospheric pressure and wind speed, to other models that need this data as a boundary forcing term. The coupler must also do additional, computationally significant work, such as interpolate the data onto a different grid. In this study, the master nodes of each model and coupler are connected and they communicate each other at every 20 seconds model time. The Multiple Program Multiple Data (MPMD) method programming was performed to couple the models. The coupler and each models united by the separated group, and they calculated by the group unit. Also they passed message when exchanging data by global unit. The data are exchanged every 20-second model time that is the least common multiple time of the atmosphere model and the ocean model.

3. Computation of The storm surge by Typhoon Bart (T9918)

In this section, we describe the application of the model to an investigation of the storm surge generated by the Typhoon Bart that struck Kyushu area on 24 September 1999 using coupled atmosphere and ocean model. This model simulates the period during the typhoon through Kyushu area from 09 JST 22 September (00 UTC 22) to 21 JST 24 September (12 UTC 22).

3.1 *Computation of wind and atmospheric pressure fields at sea surface*

Figure 6 shows the track and central pressure (in hPa) of the Typhoon Bart based on the JMA track data. Using the data, the atmosphere model was executed in the period from 09 JST 22 September to 21 JST 24 September, 1999 with coupling system. The predicted typhoon track (dotted line) is similar to JMA track data (solid line) before typhoon landed Kyoshu area. Also the ocean model simulated standalone mode during same period without atmospheric forcing to predict the astronomical tides and allow the surge component to be derived.

Figure 7 shows the surface pressure and wind barbs (plotted for every 10th grid point of the model within the computational domain) at 05 JST 24 September. The wind barbs spiral and converge cyclonically towards the center of the typhoon. A well-defined and asymmetric region of maximum wind speed greater than 30 m/s was produced around the eye. The maximum wind speed (> 40m/s) was simulated in the southeast quadrant of the storm.

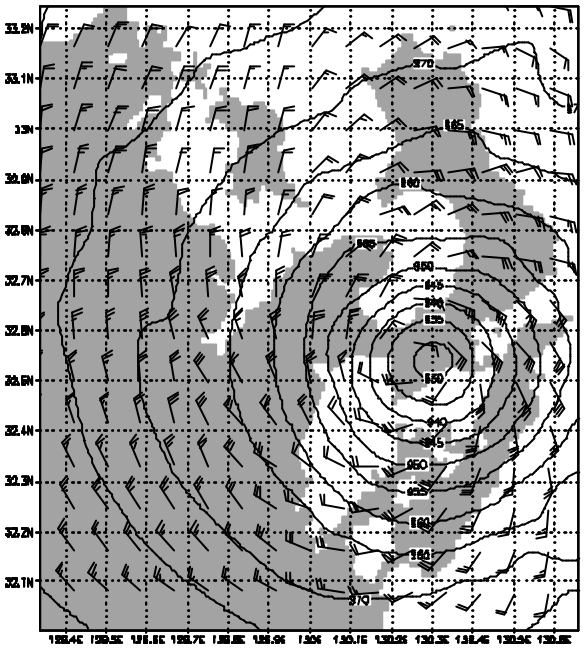

Figure 7. Computed atmospheric pressure (contours) and wind fields (barbs) at 05 JST 24 September by MM5, which are input of external forces to POM. One full feather in the barb indicates the wind speed of 10 m/s.

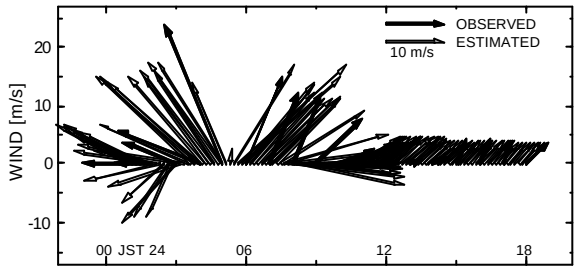

Figure 8. Model and observation wind vectors at Yatsushiro Harbour.

Figure 8 shows the wind vector observed and estimated at Yatsushiro Harbour, where the filled arrow indicates the observed mean wind speed and direction and unfilled arrow indicates the computed mean speed and direction of surface wind computed by MM5. Observed wind data is plotted every 1 hour and computed wind data is plotted every 10 minutes. Although the strong wind at 05 JST 24 September observed toward northwest about 30m/s speed, the computed wind is almost disappeared. The simulated typhoon moves closely near Yatsushiro Harbour that observed data. It is the reason why computed wind is near the eye resulting in weak wind at 05 JST. As a consequence, MM5 shows the strong wind at 04 JST toward northwest and 07 JST toward northeast. Wind

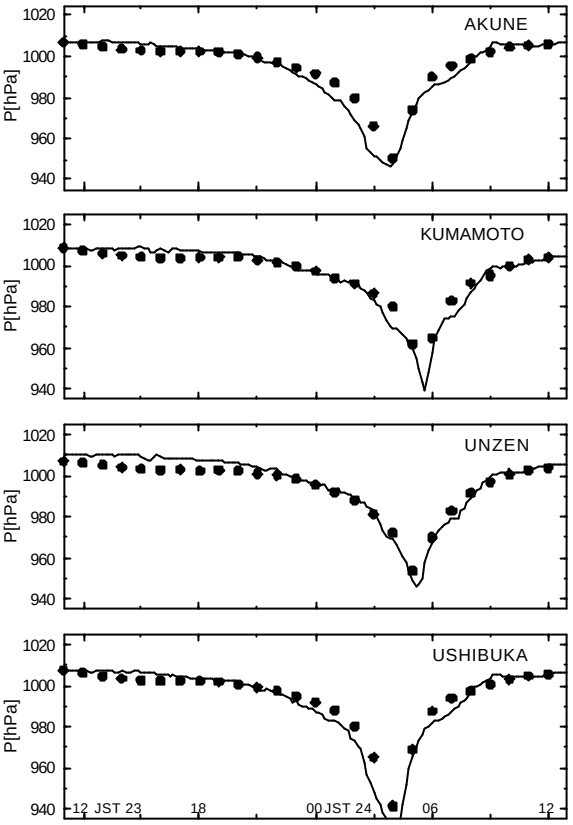

Figure 9. Time series of the observed (circles) and calculated (lines) atmospheric pressure.

data observed at Yatsushiro Harbour affected by land topography of Kyushu Island. Contrary to the simple typhoon model, MM5 could consider realistic terrain and physical effect.

Figure 9 shows the observed pressure in the JMA's meteorological observation stations, Akune, Kumamoto, Unzen and Ushibuka, and computed sea level pressure. The sea level pressure computed MM5 seems to overestimate compared observed data.

3.2 *Tide computation in the Ariake Sea*

The tide of the Ariake and Yatsushiro Seas is characterized by very large difference of tidal height and strong tidal current. The amplitude and phase of the tidal elevation were calculated by the harmonic decomposition from the elevation results of each constituent case run. Totally 8 constituents are computed and verified by tidal harmonic constant published by the Japan Coast Guard. The real-time tide simulation was computed by composing the tidal boundary condition of the 8 constituents. The comparison of time series with observed and computed sea level elevation from 12 JST 23

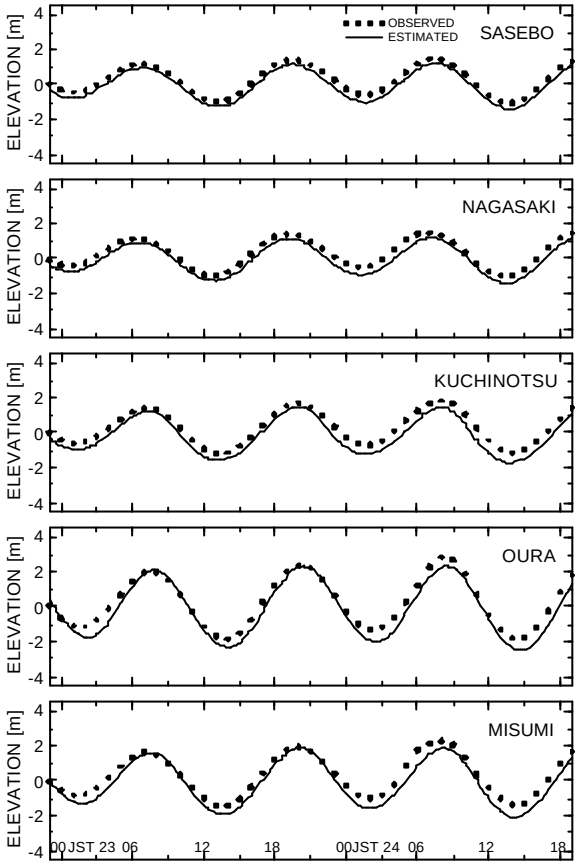

Figure 10. Comparison between observed (circles) and predicted (lines) astronomical tides.

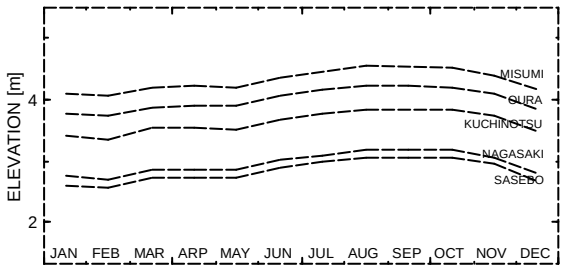

Figure 11. Monthly averaged mean sea level in 1999.

September to 12 JST 24 September, 1999 at Sasebo, Nagasaki, Kuchonotsu, Oura and Misumi (Figure10). Observed data is 1-hour interval tidal gage data from Japan Oceanographic Data Center (JODC). The elevation difference is shown in the comparison chart that caused by the seasonal effect. Figure 11 shows the seasonal change the mean sea level at 5 tidal gage stations. The MSL during 1 year in 1999 at MISUMI is 4.31 meter, but during September is 4.52 meter. The MSL become the lowest in the winter and the highest in the Autumn within the narrow limits of seasonal average.

3.3 *Storm surge computation*

Figure 12 shows time series of the total water level (relative to MSL), the astronomical tidal elevation (also relative to MSL) and the observed storm surge elevation, defined at any time as the difference between total water level and predicted tide for Yatsushiro Harbor. It can be seen from Figure 12 that the rapidly moving typhoon produced a surge of quite short duration (6 hours). Two peaks have occurred in this observed sea level. The extreme high sea level at the 1st peak was raised by the inverted barometer effect. It is thought that the 2nd peak is *seiche* of the direction of north and south in the Yatsushiro Sea. The highest sea level elevation, 268 cm, observed at 0603 JST 24 September, 1999. The estimated sea level elevations of 263 cm and 270 cm are computed at 0540 JST 24 and 0640 JST 24.

Sea level changes at 5 stations, Yatsushiro, Matsuai, Misumi, Kuchinotsu and Oura, in the computational domain of the Ariake and Yatsushiro Seas are shown in Figure 13. It can be confirmed that the highest tide is reproduced in the northern end of the Yatsushiro Sea (Matsuai), which agrees with observed fact. The observed maximum sea surface elevation at the inner area of the Yatsushiro Sea, Matsuai, estimated 450 cm sea level but simulation could not trace it. This simulation-observation gap may come from of the wind stress formulation in the shallow water in which wind-induced breaking of shoaling waves may be enhanced by increasing of wave steepness.

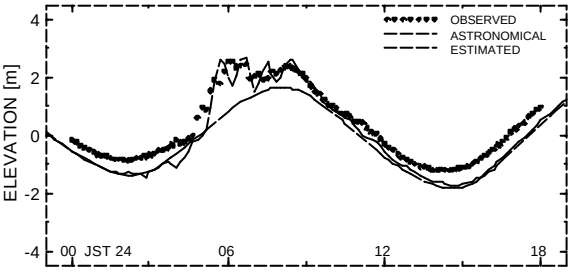

Figure 12. Observed and computed sea level changes at Yatsushiro Harbor

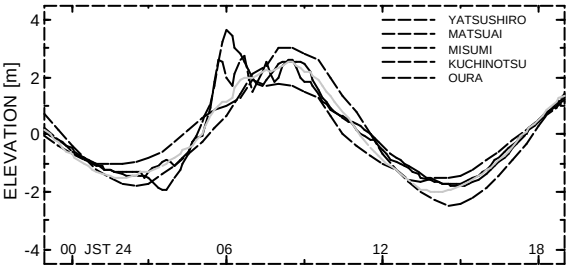

Figure 13. Computed sea surface elevations in the Ariake and Yatsushiro Seas.

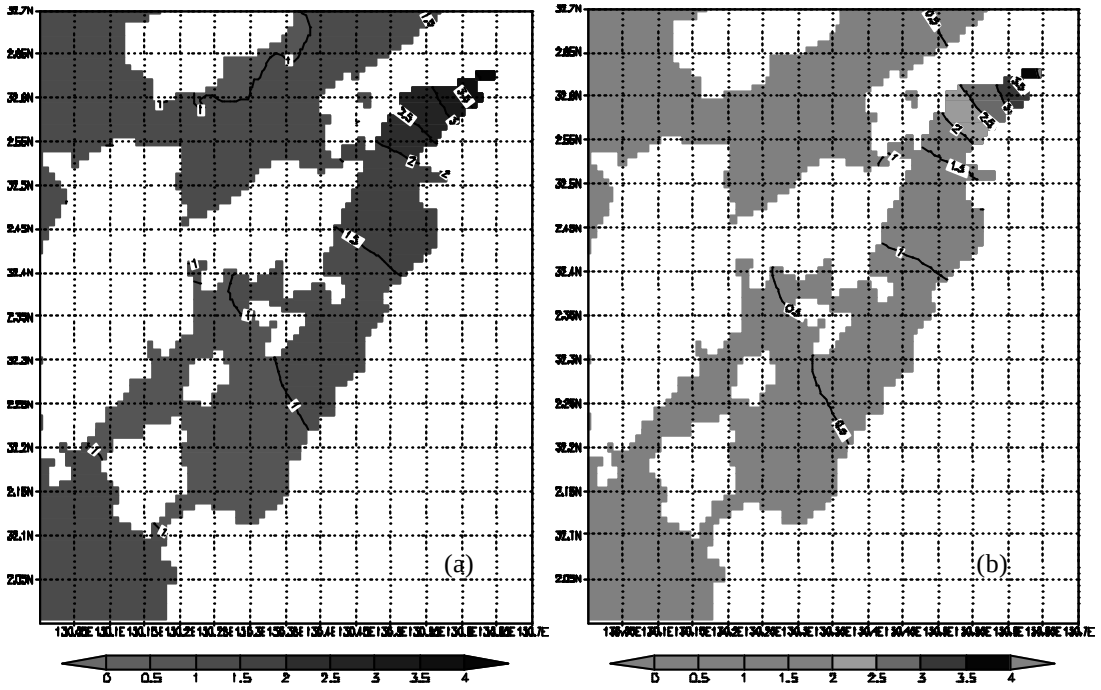

Figure 14. Distributions of (a) computed water level (m) due to tide and surge combined, (b) computed storm surge anomalies (m) without tide component, at 05 JST 24 September, 1999.

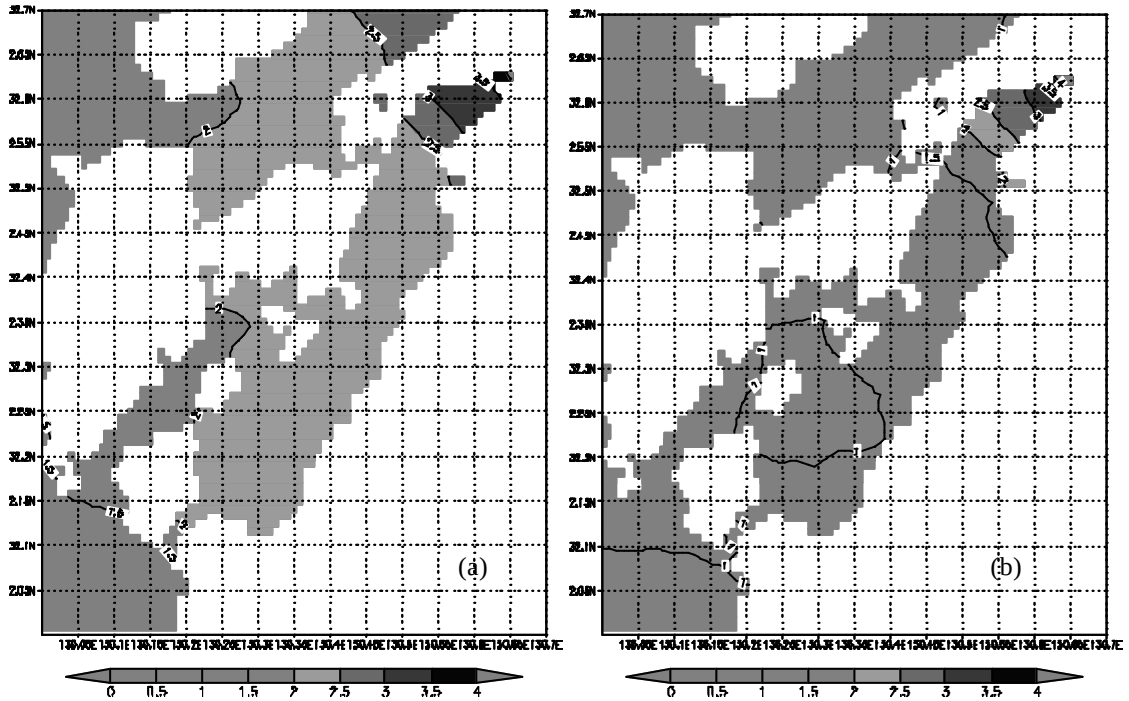

Figure 15. Distributions of (a) computed maximum water level (m) due to tide and surge combined, (b) computed maximum storm surge anomalies (m) without tide component, in the period 09 JST 23 September to 21 JST 24 September, 1999.

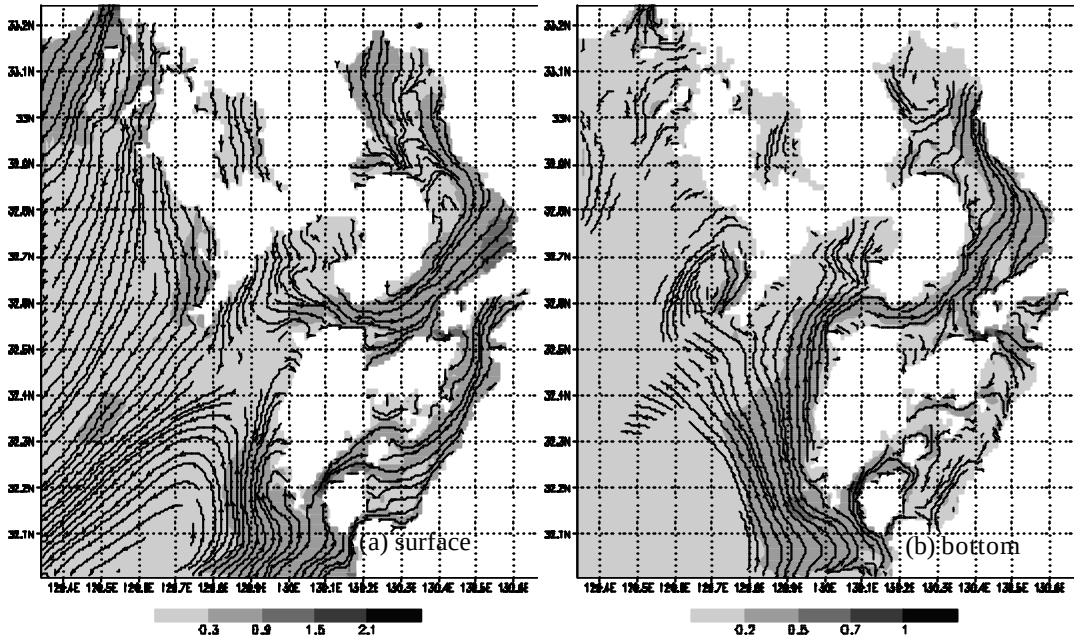

Figure 16. Distributions of (a) computed surface currents streamline and its magnitude (m/s), (b) computed bottom currents at 05 JST 24 September, 1999.

The corresponding distributions of computed water level due to tide and surge combined, and computed storm surge anomalies without tide component are shown in Figure 14a and 14b at 05 JST 24 September, 1999. Figure 15a shows the distribution of computed maximum water level due to tide and surge combined, and Figure 15b shows the distribution of computed maximum storm surge anomalies without tide component at 05 JST 24 September, 1999. The highest storm surge anomaly was 4.4 m above mean sea level (MSL) at the end of the Yatsushiro Sea, 3.23 m was calculated at north of the Ariake Sea. The distribution of surface and bottom currents caused by wind and pressure are shown in Figure 16a and 16b at 05 JST 24 September, 1999. These results are computed without tidal forcing to show only the wind and pressure effects.

4. Conclusions and future prospects

Numerical hindcast of storm surge caused by the Typhoon Bart (T9918) in Kyushu is conducted by using hydrodynamic model (POM) and mesoscale atmosphere model (MM5), and it makes the result of encouraging hindcast in sea surface elevation at the Ariake and Yatsushiro Seas. But the computed maximum sea surface elevation is lower than observed run-up height at Matsuai where the significant damage (the toll of the death was 12) due to inundation by storm surge flooding occurred.

We supposed that the simulation-observation gap in sea surface elevation at the end of the Sea may come from the wind stress formulation in the extremely shallow water, in which wind-induced breaking white caps of shoaling waves may enhance surface shear stress field by increasing of wave steepness. New formulation of the surface shear stresses as well as breaker-induced stresses may play an important role in the shallow water. To take such effect into account, we define an additional shear stress due to wave breaking on the sea surface, which is considered as shearing stress caused by surface roller of whitecap breaker, that is equivalent to the whitecap energy dissipation rate divided by the wave celerity in the wave energy flux conservation.

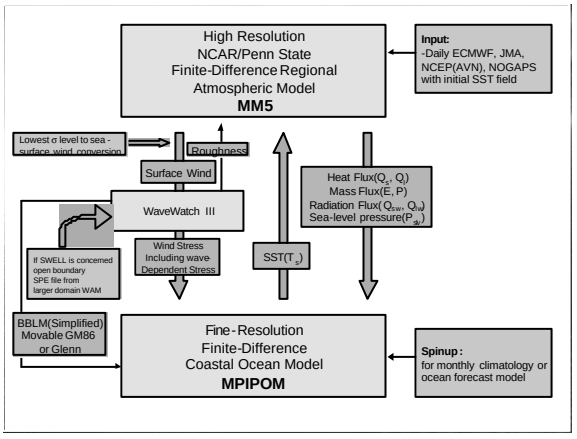

Figure 17. Coupling between the atmosphere, wave and ocean models and the relation between models.

Mastenbroek et al. (1993) show the effect of a wave-dependent drag coefficient on the generation of storm surges and exhibit that the calculations with a Smith and Banke stress relation underestimate the surges by 20% compared the coupled wave and storm surge models. We hope a more comprehensive coupled model considering air-wave-current interaction may fill this gap, and its relation between models for typhoon wind field, ocean/coastal wave, ocean tide and storm surge is schematically shown in Figure 17.

References

Fujii, T., Maeda, J., Ishida, N., and Hayashi, T. (2002). An analysis of a pressure pattern in severe Typhoon Bart hitting the Japanese Islands in 1999 and a comparison of the gradient wind with the observed surface wind, *J. Wind Eng. Ind. Aerodyn.* **90,** 1555-1568.

Grell, G. A., Dudhia, J., and Stauffer, D. R. (1994). *A description of the fifth-generation Penn State-NCAR Mesoscale Model (MM5)*, NCAR Tech. Note NCAR/TN-398+STR. 122p.

Kim, K. O., and Yamashita, T. (2002). Tidal Simulation in Ariake Sea by Parallelized Ocean Model, *Recent Advances in Marine Science and Technology* (accepted for publication).

Manda, A., and Yanagi, T. (2001). The storm surge induced by Typhoon 9918 in the Yatsushiro Sea, Japan : a comparison of Typhoon 9918 with Typhoon 9119, *J. Oceanography*. **10,** 4, 285-295.

Mastenbroek, C., Burgers, G, and Janssen, P. A. E. M. (1993) The Dynamical Coupling of a Wave Model and a Storm Surge Model through the Atmospheric Boundary Layer, *J. Phy. Ocean*. **23,** 1856-1866

Mellor, G. L. (1998). *User's Guide for a three-dimensional, primitive equation, numerical ocean model*, Princeton University, Internal Report. 40p.

Mellor, G. L., and Yamada, T. (1982). Development of a turbulence closure model for geophysical fluid problems, *Reviews of Geophysics and Space Physics*. **20,** 4, 851-875.

Reisner, J., Rasmussen, R. M., and Bruintjes, R. T. (1998). Explicit forecasting of supercooled liquid water in winter storms using the MM5 mesoscale model, *Quart. J. Roy. Meteor. Soc*. **124**, 1071-1107.

Reynolds, R. W. and Smith, T. M. (1994). Improved global sea surface temperature analyses, *J. Climate*. **7,** 929-948.

Simons, T. J. (1980). Circulation models of lakes and inland seas, *Can. Bull. Fish. Aquat. Sci.* **203**, 145.

Smith, S. D., and Banke, E. G. (1975). Variation of the sea surface drag coefficient with wind speed, *Quart. J. Roy. Meteor. Soc*. **101**, 665-673

Yamashita, T., and Nakagawa, Y. (2001). Storm surge model in the shoaling region: application to storm surge in the Yatsushiro Sea, Typhoon 9918 case, *Proc. Coastal Eng.* **48,** 291-295.

Yoshino, J., Ishikawa, H, and Ueda, H. (2002). MM5 simulations of the 24 September 1999 tornadic events in the outer rainband with Typhoon Bart (1999), *Twelfth PSU/NCAR Mesoscale Model Users' Workshop 2002*.

大気・海洋結合モデルの並列計算システムとその適用
―台風 9918 号による八代海の高潮の追算―

金　庚玉*・山下隆男

* 京都大学大学院工学研究科

要旨

メソ気象モデル（MM５），海洋モデル（POM）を連結系として数値計算する並列計算システム（Beowulf System）を構築し，八代海における台風 9918 による高潮の追算を実施し，並列計算効率，モデルの適用性に関する基礎的な検討を行った。

地上風の風域場は，簡単化された台風モデルとは異なり，陸上地形の影響が考慮された再現結果が得られた。高潮計算においては，八代港における実測値と数値シミュレーション結果とを比較し，モデルの適用性を確認した。しかし，災害の発生した湾奥の松合地区での計算最大水位は過少評価であった。これは，数値計算に風波の影響を考慮していないためであると考えられる。

キーワード：高潮，台風 9918 号，並列計算，大気・海洋結合モデル